Generic strong coupling behavior of Cooper pairs on the surface of superfluid nuclei

N. Pillet,[1] N. Sandulescu,[2,3] and P. Schuck[3,4]
[1]*DPTA/Service de Physique nucléaire, CEA/DAM Ile de France, BP12, F-91680 Bruyères-le-Châtel, France*
[2]*Institute of Physics and Nuclear Engineering, 76900 Bucharest, Romania*
[3]*Institut de Physique Nucléaire, CNRS, UMR8608, Orsay, F-91406, France*
[4]*Université Paris-Sud, Orsay, F-91505, France*
(Received 26 January 2007; revised manuscript received 18 June 2007; published 9 August 2007)

With realistic HFB calculations, using the D1S Gogny force, we reveal a generic behavior of concentration of small sized Cooper pairs (2–3 fm) in the surface of superfluid nuclei. This study confirms and extends previous results given in the literature that use more schematic approaches.

DOI: 10.1103/PhysRevC.76.024310 PACS number(s): 21.30.Fe, 21.10.Re, 21.60.Jz, 24.30.Cz

The opportunities offered by the new radioactive beam facilities to study the properties of weakly bound nuclei with large neutron skins or halos triggered new interest for the issue of space correlations induced by the formation of Cooper pairs. The spatial correlations of Cooper pairs in superfluid nuclei have not been extensively studied in the past, but nevertheless a certain number of investigations, some rather early, do exist. Mostly this was done for the single Cooper pair problem. For example the rms diameter of the extra neutron pair in ^{18}O is shown as a function of the nuclear radius by Ibarra *et al.* [1]. One sees a strong minimum in the nuclear surface, indicating a rms separation between the two active neutrons of the order of 2–3 fm. A similar behavior was found later by Catara *et al.* [2] and Ferreira *et al.* [3] for a neutron pair in ^{206}Pb and ^{210}Pb. More recently, there are also many investigations of the single Cooper pair problem in the halo nucleus ^{11}Li (see, e.g., Refs. [4,5] and citations in there).

One of the rare papers where spatial correlations of Cooper pairs are investigated in superfluid nuclei is the one of Tischler *et al.* [6] where the probability distribution of the pairs is shown as a function of the center of mass $R = \frac{1}{2}|\vec{r}_1 + \vec{r}_2|$ and the relative distance of the nucleons in the pairs $r = |\vec{r}_1 - \vec{r}_2|$ with $(\vec{r}_1, \vec{r}_2)$ the coordinates of two nucleons. They showed that in the open shell isotope ^{114}Sn one also finds Cooper pairs with short range space correlations, as in one pair systems. They also confirmed the finding of Catara *et al.*, i.e., the important role played by the parity mixing for inducing short range space correlations. Most of those older works were, however, done using rather schematic models and/or pairing forces. There exists, however, one study with a realistic pairing force (i.e., the Gogny interaction) by Barranco *et al.* [7], dedicated to nuclei embedded in a neutron gas, a system found in the inner crust of neutron stars. One of the first systematic analyses of strong dineutron spatial correlations induced by the pairing interaction was done recently by Matsuo *et al.* [8], using a zero range pairing force. The study of nuclear surface pairing properties was also the aim of several half infinite matter investigations [9,10]. It was found that the pair density reaches out further than the ordinary density but neither the local coherence length nor the probability distribution of the pairs were calculated.

The aim of the present work is to verify how much all these relatively scattered pieces of information withstand a general study of superfluid nuclei using one of the most performing HFB approaches, that is employing the finite range D1S Gogny interaction [11]. As a matter of fact we will see that many of the earlier findings are qualitatively or even quantitatively confirmed. Indeed, we will show that the strong concentration of pair probability of small Cooper pairs in the nuclear surface is a quite general and generic feature and that nuclear pairing is much closer to the strong coupling regime [8,12] than previously assumed.

We will start by explaining shortly how the spatial properties of nuclear pairing are investigated within the HFB approach and then we shall present our results and conclusions. For further understanding of the phenomena, a simple semiclassical analytic model for nuclear pairing will also be considered.

It is well known [13] that pairing correlations can be adequately studied with the Cooper-pair probability $|\kappa|^2$. The latter can be introduced by considering the two-body density matrix in the HFB approximation given by [14]

$$\begin{aligned}&\rho(\vec{r}_1 s_1, \vec{r}_2 - s_2, \vec{r}_1 s_1, \vec{r}_2 - s_2)\\ &\quad = \langle \psi^+(\vec{r}_1, s_1)\psi^+(\vec{r}_2, -s_2)\psi(\vec{r}_2, -s_2)\psi(\vec{r}_1, s_1)\rangle\\ &\quad = \rho(\vec{r}_1 s_1, \vec{r}_1 s_1)\rho(\vec{r}_2 - s_2, \vec{r}_2 - s_2) - \rho(\vec{r}_1 s_1, \vec{r}_2 - s_2)\\ &\qquad \times \rho(\vec{r}_2 - s_2, \vec{r}_1 s_1) + |\kappa(\vec{r}_1 s_1, \vec{r}_2 s_2)|^2. \qquad (1)\end{aligned}$$

In Eq. (1), $\langle \ldots \rangle = \langle \mathrm{HFB}| \ldots |\mathrm{HFB}\rangle$, ψ^+ and ψ are creation and annihilation operators, $\rho(\vec{r}_1 s_1, \vec{r}_2 s_2) = \langle \psi^+(\vec{r}_2 s_2)\psi(\vec{r}_1 s_1)\rangle$ is the single particle density matrix and $\kappa(\vec{r}_1 s_1, \vec{r}_2 s_2) = \langle \psi(\vec{r}_2 - s_2)\psi(\vec{r}_1 s_1)\rangle$ is the anomalous density matrix or pairing tensor in r-space. The first two terms on the right hand side of Eq. (1) represent the antisymmetrized mean field factorization into products of single particle density matrices which also survive in the pure Hartree-Fock limit. It is the trivial and uncorrelated part of the density matrix. The genuine two-body correlations of interest here, i.e., the pairing correlations, are contained in $|\kappa(\vec{r}_1 s_1, \vec{r}_2 s_2)|^2$.

In this paper we analyze the space properties of the pairing tensor calculated in HFB approximation, using the two-body D1S Gogny force [11]. The HFB equations are solved for spherical symmetry and using a harmonic oscillator basis. In

this framework the pairing tensor corresponding to pairs of like particles and coupled to the total spin $S = 0$ writes

$$\kappa(\vec{r}_1, \vec{r}_2)_{S=0} = \sum_s \langle \psi(\vec{r}_2 - s)\psi(\vec{r}_1 s)\rangle = \frac{1}{4\pi} \sum_{n,n'lj} \frac{2j+1}{2} \kappa^{lj}_{n',n} u_{n'l}(r_2) u_{nl}(r_1)(-)^l \times P_l(\cos\theta_{12}), \quad (2)$$

where $u_{nl}(r)$ are the radial wave functions of the harmonic oscillator and $\kappa^{lj}_{n'n}$ is the matrix of the pairing tensor for a given angular momentum lj. As defined here, the latter has an intrinsic parity $(-)^l$. In the Gogny-HFB calculations the pairing tensor has also a component with the total spin $S = 1$. Since in open shell nuclei this component is very small compared to the $S = 0$ part, it is neglected in the present study.

In order to analyze the nonlocal properties of pairing correlations, we write the pairing tensor in terms of relative and center of mass (c.m.) coordinates, i.e., $\vec{r} = \vec{r}_1 - \vec{r}_2$ and $\vec{R} = (\vec{r}_1 + \vec{r}_2)/2$. This is done by using the Brody-Moshinski transformation. One thus obtains

$$\kappa(\vec{R}, \vec{r})_{S=0} = \frac{1}{4\pi} \sum_{n,n',l_1 j_1} (2j_1 + 1)\kappa^{l_1 j_1}_{n_2,n_1} \times \sum_{nNl} (-)^l \left(\frac{2l+1}{2l_1}\right)^{1/2} u_{nl}(r/\sqrt{2}) u_{Nl}(\sqrt{2}R) \times P_l(\cos\theta)\langle nlNl; 0|n_1 l_1 n_2 l_1; 0\rangle, \quad (3)$$

where $\langle nlNl; 0|n_1 l_1 n_2 l_1; 0\rangle$ is the Brody-Moshinski bracket and θ is the angle between $\vec{r}$ and $\vec{R}$. The values of $|\kappa|^2$ and the related quantities presented below have been averaged over the angle θ. In the calculations, a basis with 15 harmonic oscillator shells have been considered.

We start by analyzing the space distribution of the pairing tensor $|\kappa(R, r)|^2$. In Figs. 1, 2, and 3 are shown the results for Sn, Ni, and Ca isotopes.

One notices a rather strong concentration of the Cooper pairs along the R-axis. However, the true extension of the Cooper pairs (r-direction) can only be judged once $\kappa(R, r)$ is properly normalized, as in the definition of its rms radius [see Eq. (4) below]. Thus, we will see that the large extensions of $|\kappa(R, r)|^2$ in the r-direction for small R-values which one can guess from Figs. 1–3, are quite important, giving rise to large coherence length values for the Cooper pairs located in the interior of nuclei. One also notices that the distribution in R is rather different for various isotopes. The difference comes from the localization properties of the single-particle

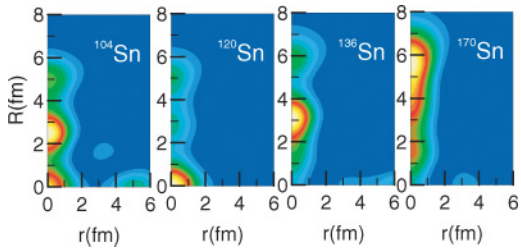

FIG. 1. (Color online) Pairing tensor $|\kappa(R, r)|^2$ for Sn isotopes.

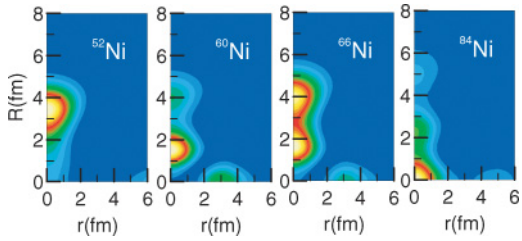

FIG. 2. (Color online) Pairing tensor $|\kappa(R, r)|^2$ for Ni isotopes.

states which are the closest to the chemical potential. For example, the pronounced concentration of $|\kappa(R, r)|^2$ around $R = 2.5$ fm in ^{104}Sn is due to the surface localization of the single-particle wave function $2d_{5/2}$, which is the closest state to the chemical potential for this isotope. One can also see that in ^{120}Sn the pair probability has a sizable value for small values of R, which comes mainly from the contribution of the state $3s_{1/2}$ to pairing correlations. On the other hand, in the isotopes $^{136-170}$Sn, $^{52-66}$Ni, and $^{44-62}$Ca, in which there is no s-state in the major shell, we see a depression of pair probability at the origin. Therefore, the distribution of Cooper pairs in nuclei is a subtle question as it depends rather strongly on the shell structure (see also [15]).

The fact that the Cooper pairs with small size are concentrated in the surface can be seen from the dependence of the coherence length on the center of mass of the pairs. The local coherence length is defined as

$$\xi(R) = \frac{\left(\int r^4 |\kappa(R, r)|^2 dr\right)^{1/2}}{\left(\int r^2 |\kappa(R, r)|^2 dr\right)^{1/2}}. \quad (4)$$

It is shown for Sn, Ni, and Ca isotopes in Figs. 4, 5, and 6.

One sees well defined and pronounced minima at $\xi \sim 2$–3 fm for R of the order of the surface radius. As we have already mentioned, a small coherence length in the case of a single Cooper pair has already been found previously for ^{18}O in Ref. [1]. It is also the case for the Cooper pair in ^{11}Li [4,5]. Our calculations did not allow to go much beyond the minima because of the employed harmonic oscillator basis which becomes inaccurate far outside the nuclear radius. However, the position of the minima is always clearly identified and seen to be similar in all cases. What is surprising is that the size of the Cooper pairs starts to decrease already well inside, around $R = 2$ fm. Moreover, the decrease toward the surface is approximately linear.

In order to get a better understanding of the structure of the local coherence length, it is appropriate to consider the locally normalized pairing tensor, as it enters in the definition of the

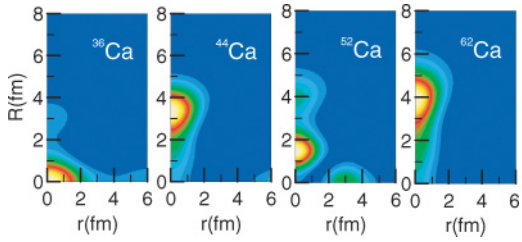

FIG. 3. (Color online) Pairing tensor $|\kappa(R, r)|^2$ for Ca isotopes.

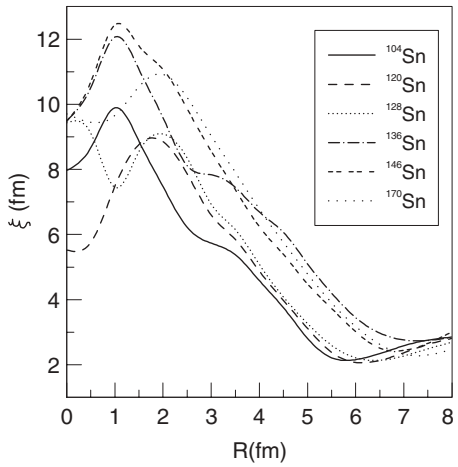

FIG. 4. Coherent length $\xi(R)$ for Sn isotopes.

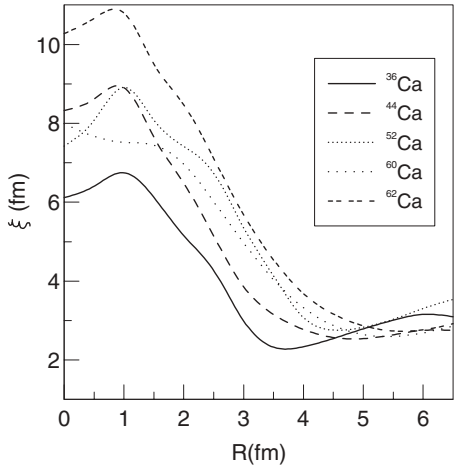

FIG. 6. Coherent length $\xi(R)$ for Ca isotopes.

coherence length [Eq. (4)], that is

$$W(R,r) \equiv r^2\kappa(R,r)^2/\mathcal{N}(R), \tag{5}$$

where $\mathcal{N}(R) = \int dr r^2 \kappa(R,r)^2$. This quantity is shown in Fig. 7 for ^{120}Sn, which presents common features seen in all analyzed isotopes. One clearly notice the large extension of the pair close to the center of the nucleus. One can also notice a rather linear decrease of the extension of the pairs toward the surface, where $W(R,r)$ has the highest concentration. How the radial structure $W(R,r)$ looks like for various values of R is shown in Fig. 8. A very typical and generic feature is revealed there. At high particle densities, i.e., close to saturation, the pair tensor function strongly oscillates with a wide extension. Going to lower densities, i.e., toward the surface, these oscillations die out and a compact structure appears. Such behavior have been pointed out in infinite matter studies [16] and also for finite nuclei [5]. The oscillatory behavior is well understood as an effect of the orthogonalization of the pair tensor function with the remaining Fermi sea. For infinite systems this behavior is known since long in condensed matter physics [17]. That there is qualitatively the same behavior in finite nuclei is somewhat a surprise, although it has been seen for the one Cooper pair problem [5]. It seems to be a quite generic behavior for all kinds of paired Fermi systems, be they homogeneous, inhomogeneous, or finite.

Next we shall discuss the probability distribution of pairing correlations defined by

$$P(R,r) = R^2 r^2 |\kappa(R,r)|^2. \tag{6}$$

This quantity is important because it enters in the calculation of the mean value of two-body operators, as pairing energy or spectroscopic factor used in the evaluation of cross sections for two-neutron transfer reactions. The results for $P(R,r)$ are shown in Figs. 9, 10, and 11 for Sn, Ni, and Ca isotopes. The striking feature is that for all nuclei the same scenario emerges: the probability distribution $P(R,r)$ is strongly concentrated in the surface with a diameter of 2–3 fm, along the isotopic chain. This effect is not practically dependent on the exoticity of nuclei. This fact explains why one finds in all superfluid nuclei a high probability for two-neutron transfer reactions.

In order to demonstrate that the strong concentration of small Cooper pairs in the surface of the nuclei is not a trivial effect, we decompose $\kappa(R,r)$ in a part $\kappa_e(R,r)$ which contains

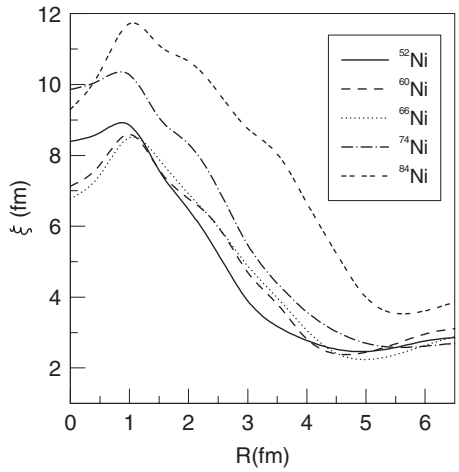

FIG. 5. Coherence length $\xi(R)$ for Ni isotopes.

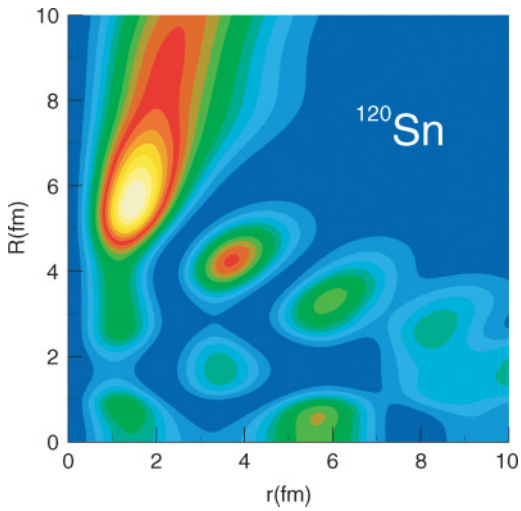

FIG. 7. (Color online) $W(R,r)$ for ^{120}Sn.

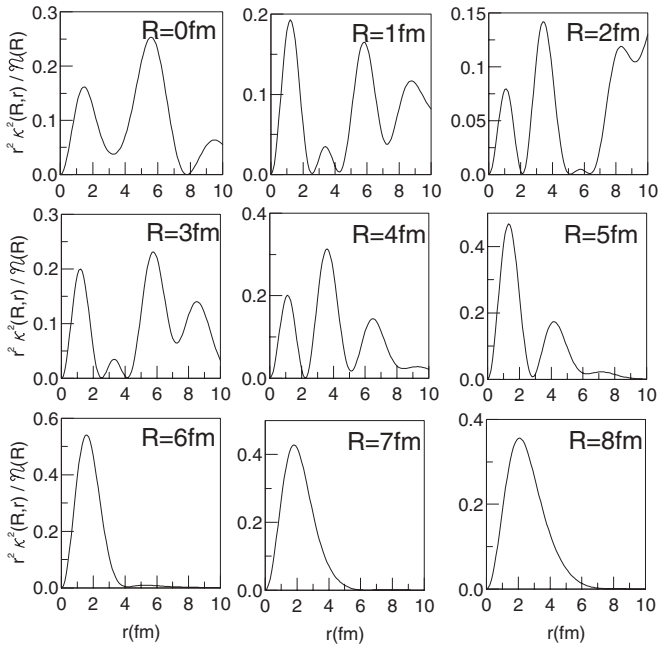

FIG. 8. $W(R, r)$ for given values of R in the case of ^{120}Sn.

only even parity wave functions and a part $\kappa_o(R, r)$ which contains only the odd parity ones, i.e., $\kappa(R, r) = \kappa_e(R, r) + \kappa_o(R, r)$. In Fig. 12, we show what are the corresponding probability distributions for $P_e(R, r)$, $P_o(R, r)$, and $P_{eo}(R, r)$ in the case of ^{120}Sn. The quantity $P_{eo}(R, r)$ corresponds to the interference term $2\kappa_e\kappa_o$. From Fig. 12, one can see that selecting only either even or odd parity states in $\kappa(R, r)$ has a strong delocalization effect on the Cooper pairs: they are democratically distributed with respect to an interchange of R and r variables [one should notice that in Eq. (3) the symmetry between R and r involves a factor 2, which comes through the standard definition of Brody-Moshinsky transformation]. So no small Cooper pairs in the nuclear surface are preferred at all in those cases. The concentration only shows up when even

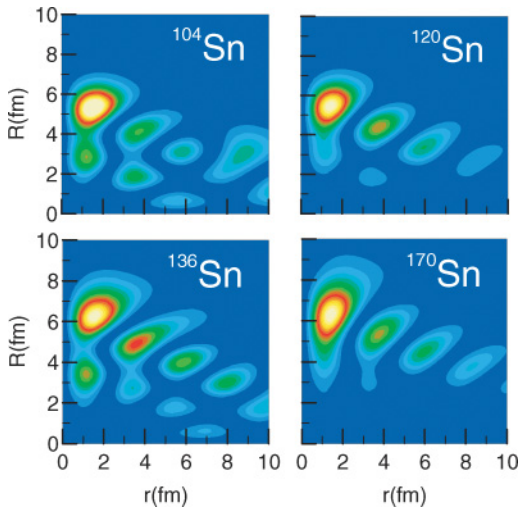

FIG. 9. (Color online) Probability distribution $P(R, r)$ for Sn isotopes.

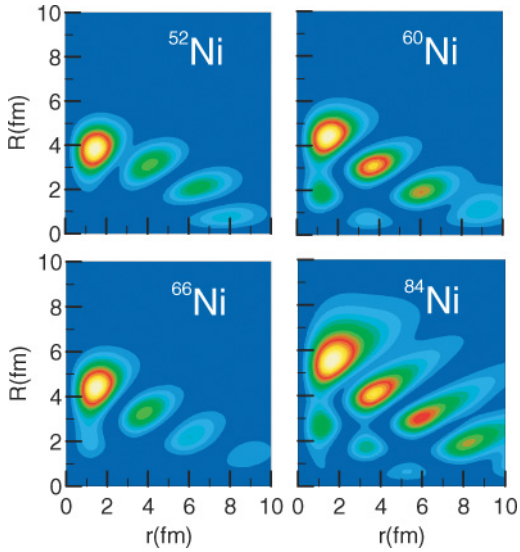

FIG. 10. (Color online) Same as Fig. 9 for Ni isotopes.

and odd parity states are mixed. This is clearly revealed in looking at the interference term $P_{eo}(R, r)$. We see that it is negative for regions close to the r-axis and positive close to the R-axis. We checked that this scenario stays the same for all other superfluid nuclei considered.

The parity mixing scenario is also well described in the papers by Catara *et al.* [2] and Tischler *et al.* [6]. Mixing of parities naturally occurs in heavy nuclei because of the presence of intruder states of unnatural parity in the main shells of given parity. However, the concentration of Cooper pairs can also occur in light nuclei as the oxygen isotopes where no intruders are present in the valence shell. This means that pairing in nuclei is sufficiently strong so that κ contains contributions from several main shells, allowing for parity mixing even in light nuclei. If one artificially restricted the pairing configurations, e.g., in ^{22}O to the *s-d* shell, then certainly no concentration effect at all would be seen (in this respect, see also the study in [6]). So to grasp the full

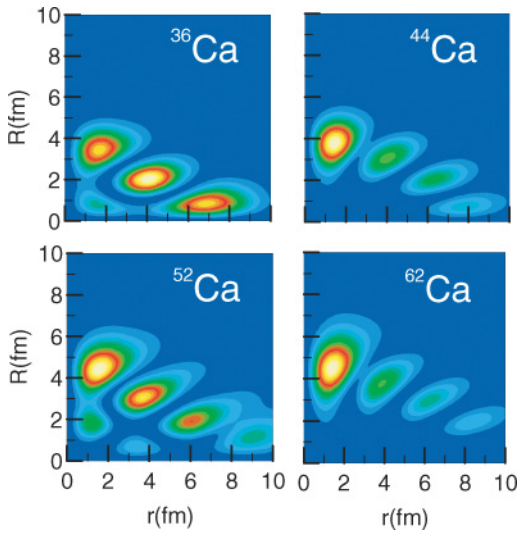

FIG. 11. (Color online) Same as Fig. 9 for Ca isotopes.

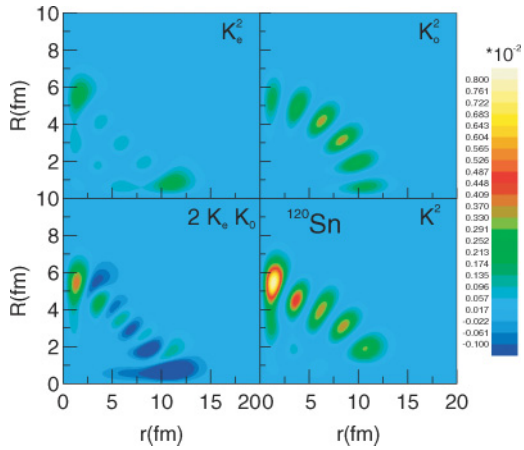

FIG. 12. (Color online) Contributions of definite parity to $P(R, r)$ calculated with HFB-D1S for ^{120}Sn.

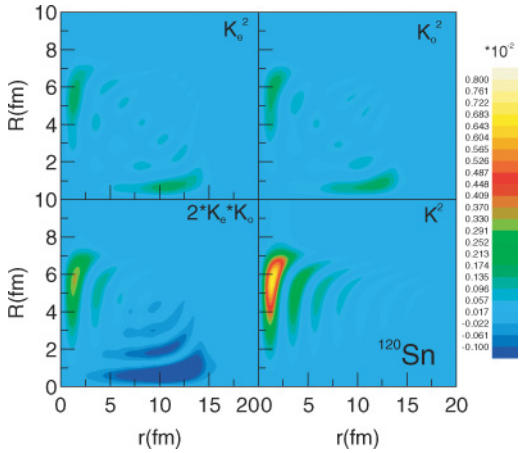

FIG. 13. (Color online) Parities contributions $P^{sc}(R, r)$ calculated with the semiclassical model for ^{120}Sn.

physics of nuclear pairing it is very important to work in a large configuration space, comprising several shells below and above the active one (see also [8]). The only exception to parity mixing we found for the analysed isotopes concerns ^{36}Ca. In this nucleus the presence of two additional neutrons in the $2s_{1/2}$ state strongly inhibits the parity mixing with the p states of the lower major shell.

In order to understand in more detail where this extraordinary concentration effect from even-odd parity mixing comes from, let us consider a very simple model. We got inspired by the Thomas-Fermi model presented in Ref. [3] where the anomalous density matrix is given by $\kappa^{TF}(R, r) \sim k_F(R) j_0(k_F(R)r)$ with $j_0(x)$ a spherical Bessel function, $k_F(R) = \sqrt{\frac{2m}{\hbar^2}(\mu - V(R))\Theta(\mu - V)}$ the local Fermi momentum, μ the chemical potential (or Fermi energy), and $V(R)$ a phenomenological mean field potential. It can be shown [18] that a slightly more elaborate semiclassical version can be written as

$$\kappa^{sc}(R, r) = \frac{m}{\hbar^2 \pi^2} \int dE \kappa(E) k_E(R) j_0(k_E(R) r), \qquad (7)$$

where $k_E(R)$ is the local momentum at energy E, obtainable from k_F in replacing μ by E, and $\kappa(E)$ is the continuum version of the κ's for the individual quantum levels: $\kappa(E) = \Delta(E)/(2\sqrt{(E-\mu)^2 + \Delta(E)^2})$. We see that for very small $\Delta's$, one gets back the TF model [3]. However, for realistic gap values the distribution of κ's is very important, otherwise the concentration effect will not show up. For $\Delta(E)$ we adjust a Fermi function to represent on average the gap-values of the individual single particle levels. An example can be seen on Fig. 12 of Ref. [19]. In the present work, we have fitted the function $\Delta(E)$ on HFB-D1S results for ^{120}Sn. A good fit function is given by $\Delta(E) = 4/[1 + \exp(E - \mu)/20]$ (all numbers are in MeV). For the mean field potential $V(R)$ we take the Woods-Saxon form of Ref. [20]. The chemical potential μ is determined, as usual, via the particle number condition.

In Fig. 13, we show the corresponding semiclassical probability $P^{sc}(R, r)$. We see qualitatively good agreement with the quantal HFB results, for instance in what concerns the concentration of small Cooper pairs in the surface. We also show in Fig. 13 the parity projected probabilities. As in Fig. 12, one sees the strong delocalization effect. In our model this can be understood analytically. Parity projection can be written as $\kappa_{e/o}(\vec{r}_1, \vec{r}_2) = \frac{1}{2}[\kappa(\vec{r}_1, \vec{r}_2) \pm \kappa(\vec{r}_1, -\vec{r}_2)] = \frac{1}{2}[\kappa(\vec{R}, \vec{r}) \pm \kappa(\frac{\vec{r}}{2}, 2\vec{R})]$ (see Ref. [21]). We therefore see that good parity implies, up to a scale factor, a symmetrisation in coordinates R and r. This is general and can be investigated analytically in the TF model.

The analytic model also allows to quickly grasp the significance of the coordinates used by Matsuo *et al.* [8]. There, one takes a reference particle at position $\vec{r}_1$ on the z-axis, i.e., $\vec{r}_1 = z_1 \vec{e}_z$. Moving the second particle on the z-axis we see that for $P_{e/o}$ two symmetric peaks at $\vec{r}_2 = z_1 \vec{e}_z$ and $\vec{r}_2 = -z_1 \vec{e}_z$ appear whereas for the total probability only one peak on the side of the test particle appears. This is a clear signature of strong pairing correlations as also pointed out in [8].

Finally we shall discuss shortly the global properties of the pair tensor distribution. The value of $|\kappa|^2$ integrated over the whole space is commonly associated to the number of correlated pairs [24]. Thus, for the isotopes ^{104}Sn, ^{120}Sn, and ^{128}Sn this number is equal to 2.09, 9.61, and 3.14. One can notice that for the first two isotopes the number of correlated pairs stays close to the number of pairs which can be formed with the valence neutrons in the shell $N = 50$–82 while for ^{128}Sn this number is closer to the half of the number of holes in the closed shell $N = 82$.

In conclusion, we showed that Cooper pairs in superfluid nuclei preferentially are located with small size (2–3 fm) in the surface region. There, they maximally profit from the Cooper phenomenon, that is, with respect to the neutron-neutron virtual S-state in the vacuum (rms 12 fm [5]), strong extra binding occurs, as long as the density is not too high. Further to the center of the nucleus the stronger effect of the orthogonalization of the pair with respect to the denser core-neutrons perturbs the pair wave function. It starts to oscillate and expands again [5]. That this simple, physically appealing and generic picture, is so pronounced, has come as a surprise. It is certainly important for the interpretation of pair transfer reactions. Most of these facts had already been revealed in the

past for specific examples and schematic models and forces. We think, it is the merit of this work that it demonstrates with realistic HFB calculations using the finite range D1S force the generic aspect of strong coupling features of singlet isovector pairing in nuclei. These features are in agreement with the ones recently put forward by Matsuo *et al*. [8]. Let us mention that the strong coupling features revealed here are somewhat contrary to the old belief [22] that the coherence length of nuclear pairs is of the same order or larger than the nuclear diameter. On the contrary, a much more diverse local picture has emerged. This may also be the reason for the rather good success of LDA for nuclear pairing found in the past [23]. In spite of the strong coupling aspects revealed in this work, we hesitate to say that there is Bose-Einstein condensation (BEC) of isovector Cooper pairs, since this, strictly speaking, occurs only for (in infinite matter) negative chemical potential, what means true binding. However, μ never turns negative for isovector pairing in infinite nuclear or neutron matters. Nuclear isovector pairing is just in the transition region from BEC to BCS.

ACKNOWLEDGMENTS

We would like to thank J. Dukelsky and S. Pittel for valuable discussions and Marc Dupuis for his help in dealing with the spherical HFB code using D1S Gogny force [11].

[1] R. H. Ibarra, N. Austern, M. Vallieres, and D. H. Feng, Nucl. Phys. **A288**, 397 (1977).
[2] F. Catara, A. Insolia, E. Maglione, and A. Vitturi, Phys. Rev. C **29**, 1091 (1984).
[3] L. Ferreira, R. Liotta, C. H. Dasso, R. A. Broglia, and A. Winther, Nucl. Phys. **A426**, 276 (1984).
[4] G. F. Bertsch and H. Esbensen, Ann. Phys. (NY) **209**, 327 (1991); H. Esbensen, G. F. Bertsch, and K. Hencken, Phys. Rev. C **56**, 3054 (1999).
[5] K. Hagino, H. Sagawa, J. Carbonell, and P. Schuck, Phys. Rev. Lett. **99**, 022506 (2007).
[6] M. A. Tischler, A. Tonina, and G. G. Dussel, Phys. Rev. C **58** 2591 (1998).
[7] F. Barranco, R. A. Broglia, H. Esbensen, and E. Vigezzi, Phys. Rev. C **58**, 1257 (1998).
[8] M. Matsuo, K. Mizuyama, and Y. Serizawa, Phys. Rev. C **71**, 064326 (2005).
[9] M. Farine and P. Schuck, Phys. Lett. **B459**, 444 (1999).
[10] M. Baldo, U. Lombardo, E. Saperstein, and M. Zverev, Phys. Lett. **B459**, 437 (1999).
[11] J. Dechargé and D. Gogny, Phys. Rev. C **21**, 1568 (1980); J.-F. Berger, M. Girod, and D. Gogny, Comput. Phys. Commun. **63**, 365 (1991).
[12] M. Baldo, U. Lombardo, and P. Schuck, Phys. Rev. C **52**, 975 (1995).
[13] P. Ring and P. Schuck, *The Nuclear Many-Body Problem* (Springer-Verlag, Berlin, 1980).
[14] D. Pines and P. Nozieres, *Theory of Quantum Liquids* (Addison-Wesley, Reading, MA, 1990), Vol. 2.
[15] N. Sandulescu, P. Schuck, and X. Vinas, Phys. Rev. C **71**, 054303 (2005).
[16] M. Baldo, U. Lombardo, and P. Schuck, Phys. Rev. C **52**, 975 (1995); M. Matsuo, *ibid*. **73**, 044309 (2006).
[17] A. L. Fetter and J. D. Walecka, *Quantum Theory of Many-Particle Systems* (McGraw-Hill, New York, 1971).
[18] X. Viñas *et al*. (in preparation).
[19] P. Schuck and K. Taruishi, Phys. Lett. **B385**, 12 (1996).
[20] S. Shlomo, Nucl. Phys. **A539**, 17 (1992).
[21] X. Viñas, P. Schuck, M. Farine, and M. Centelles, Phys. Rev. C **67**, 054307 (2003).
[22] A. Bohr and B. R. Mottelson, *Nuclear Structure* (Benjamin, Reading, MA, 1975).
[23] H. Kucharek, P. Ring, P. Schuck, R. Bengtsson, and M. Girod, Phys. Lett. **B216**, 249 (1989).
[24] C. N. Yang, Rev. Mod. Phys. **34**, 694 (1962); G. Ortiz and J. Dukelsky, Phys. Rev. A **72**, 043611 (2005).